Journal of Alloys and Compounds 506 (2010) 488–491

Contents lists available at ScienceDirect

Journal of Alloys and Compounds

journal homepage: www.elsevier.com/locate/jallcom

Spin-glass-like behavior in rhombohedral $Li[Li_{(1/3-x/3)}Mn_{(2/3-2x/3)}Ni_x]O_2$ ($x = 0.4$)

Hong Chen[a,b], Lina Liu[c], Zhe Li[a], Yingjin Wei[c], Xing Meng[c], Chunzhong Wang[c], Gang Chen[c], Fei Du[c,*]

[a] College of Materials Science and Engineering, Jilin University, Changchun, PR China
[b] College of Physics, Beihua University, Jilin, PR China
[c] College of Physics, State Key Laboratory of Superhard Materials, Jilin University, Changchun, PR China

ARTICLE INFO

Article history:
Received 16 March 2010
Received in revised form 30 June 2010
Accepted 8 July 2010
Available online 15 July 2010

Keywords:
$Li[Li_{0.2}Mn_{0.4}Ni_{0.4}]O_2$
Spin-glass-like

ABSTRACT

The magnetic properties of $Li[Li_{(1/3-x/3)}Mn_{(2/3-2x/3)}Ni_x]O_2$ ($x = 0.4$) are investigated by *dc* magnetization measurements. The high-temperature paramagnetic susceptibility can be fitted by Curie–Weiss law whose Curie and Weiss constants are 0.95(2) emu K/mol Oe and −70(4) K, respectively. The ZFC/FC curves of $Li_{0.2}Ni_{0.4}Mn_{0.4}O_2$ show a strong irreversibility behavior and T_{irr} shifts to lower temperature with the increase of applied magnetic field. Together with de Almeida–Thouless (AT) line analysis, spin-glass-like state is suggested to be the ground state of $Li_{0.2}Ni_{0.4}Mn_{0.4}O_2$. In addition, the frustration parameter $|\theta|/T_f$ is calculated to be about 7.8, lower than the value that frustration effect is strong enough to give rise to spin-glass behavior. It is concluded that the spin-glass-like behavior results from the short-range structure disorder rather than the geometrical frustration.

1. Introduction

Layered $Li[Li_{(1/3-x/3)}Mn_{(2/3-2x/3)}M_x]O_2$ (M = Co, Ni and Cr) oxides have attracted much attention as cathode materials for lithium ion batteries [1–4]. Layered $Li[Li_{(1/3-x/3)}Mn_{(2/3-2x/3)}M_x]O_2$ can usually be considered to be the solid solutions of two layered materials, $LiMO_2$ (M = Co, Ni and Cr) and $Li(Li_{1/3}Mn_{2/3})O_2$. In rhombohedral $LiMO_2$ (space group $R\bar{3}m$) compound, the average oxidation state of M is +3 and Li and M ions occupy 3a and 3b sites in separated layers. In contrast monoclinic $Li(Li_{1/3}Mn_{2/3})O_2$ (space groupC2/*m*) can be regarded as lithium-rich material and part lithium and manganese ions both comprise the transition metal layer. Although the variation in crystallographic space group symmetry may bring about some differences in electronic configurations, the close-packed layers in each of these compounds [(0 0 1) in monoclinic $Li(Li_{1/3}Mn_{2/3})O_2$ and (0 0 3) in rhombohedral $LiMO_2$] have the similar interlayer spacing close to 4.7 Å [4]. This compatibility of the close-packed layers allows the integration of a Mn_2O_3 component with a MO_2 component at the atom level, which allows for some disorder arrangement between Mn and M cations [4].

Layered $Li[Li_{(1/3-x/3)}Mn_{(2/3-2x/3)}\ M_x]O_2$ (M = Co, Ni and Cr) oxides shows better electrochemical performance than rhombohedral $LiMO_2$ due to the structure stabilization during cycling [1–6]. For example, $Li[Li_{(1/3-2x/3)}Mn_{(2/3-x/3)}Ni_x]O_2$ shows high capacity more than 200 mAh/g between 2.0 and 4.8 V and good cycling performance [1]. Many of the electrochemical properties of interest, such as charge capacity and capacity retention upon cycling, are closely related to cation ordering [7–10]. It has been predicted theoretically that spin-glass transition should be observed in the geometrical frustrated antiferromagnetism with weak disorder [11]. Considering the equilateral triangle sublattice of transition metal layers and disorder arrangement between Mn and M cations, spin glass may be the possible ground state of $Li[Li_{(1/3-x/3)}Mn_{(2/3-2x/3)}M_x]O_2$. In this article, we prepared $Li[Li_{(1/3-x/3)}Mn_{(2/3-2x/3)}M_x]O_2$ with $x = 0.4$ by citrate precursor method and studied the magnetic properties by employing *dc* magnetization measurements.

2. Experiments

The powder sample was prepared using lithium hydroxide [$LiOH{\cdot}H_2O$], nickel acetate [$Ni(CH_3{-}COO)_2{\cdot}4H_2O$] and manganese acetate [$Mn(CH_3{-}COO)_2{\cdot}4H_2O$] as the starting materials. For the first step, stoichiometric amount of starting materials were dissolved 100 mL distilled water. Then added dropwise to a 0.5 mol L^{-1} citric acid aqueous solution with constant stirring at 70–80 °C for 4–6 h. The resultant solution was then dried at 120 °C to get a solid precursor. This solid precursor was milled to a fine powder, and then pre-treated at 450 °C in muffle furnace for 5 h. The as-prepared was then grounded and subjected to calcinations at 900 °C for 10 h at the ambient condition to obtain the final products.

The crystal structure of the sample was studied by X-ray diffraction on a Bruker AXS diffractometer with a Cu Kα radition. The diffraction data was recorded in the 2θ range of 10–70° with a step of 0.01°. Magnetic characterization was performed by a superconducting quantum interference device magnetometer (Quantum Design MPMS-XL).

* Corresponding author. Tel.: +86 431 85155126; fax: +86 431 85155126.
E-mail address: dufei@jlu.edu.cn (F. Du).

0925-8388/$ – see front matter © 2010 Elsevier B.V. All rights reserved.
doi:10.1016/j.jallcom.2010.07.044

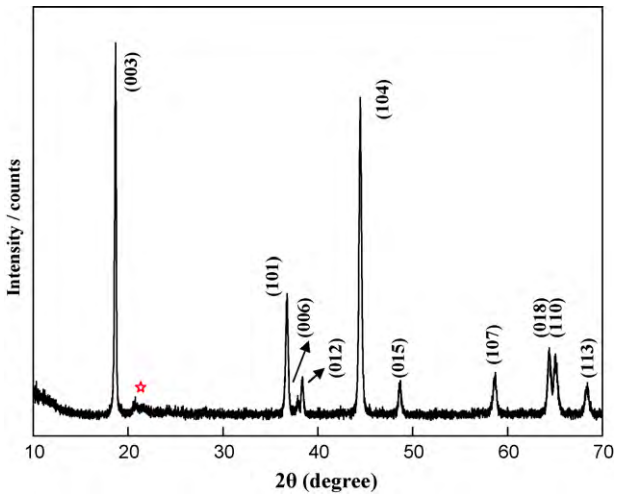

Fig. 1. Powder XRD pattern at room temperature for $Li[Li_{0.2}Mn_{0.4}Ni_{0.4}]O_2$.

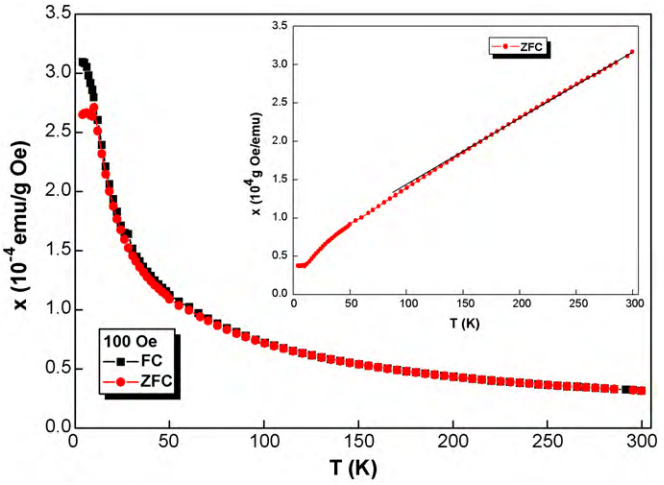

Fig. 2. ZFC and FC susceptibility as a function of temperature between 4 K and 300 K in an applied magnetic field of 100 Oe. The inset shows the reciprocal susceptibility, including a Curie–Weiss law fitting to the data above 200 K.

3. Results and discussion

A powder XRD pattern for $Li[Li_{0.2}Mn_{0.4}Ni_{0.4}]O_2$ is presented in Fig. 1. The diffraction peaks marked by "*" are attributed to the superlattice ordering in the transition metal layer, which has been considered as the typical feature of $Li[Li_{(1/3-x/3)}Mn_{(2/3-2x/3)}M_x]O_2$ (M = Co, Ni and Cr) system [1–6]. Except for the superlattice peaks, most of the diffraction peaks can be indexed to the rhombohedral α-$NaFeO_2$ structure with space group $R\bar{3}m$. The lattice parameters of the sample are calculated to be $a = 2.8693$ Å and $c = 14.2217$ Å by least-squares refinement method, in good agreement with the previously reports [3,4].

Temperature dependence of the zero-field cooled (ZFC) and field cooled (FC) magnetizations in an applied field of 100 Oe for $Li[Li_{0.2}Mn_{0.4}Ni_{0.4}]O_2$ are shown in Fig. 2, together with the reciprocal ZFC/FC curves. The ZFC/FC curves increase with the decrease of temperature and exhibits a pronounced broad peak at about 10 K in ZFC branch, which is reminiscent of the behavior of spin glass. As shown in the inset of Fig. 2, the high-temperature region of reciprocal ZFC curve can be well fitted by Curie–Weiss law $x = C/T - \theta$, where x is the susceptibility, C is Curie constant and θ is Weiss constant [12]. The Weiss constant are calculated to be −70(4) K which indicates strong antiferromagnetic interaction. The Curie constant is 0.95(2) emu K/mol Oe with which the effective moment $\mu_{eff} = 2.75(3)\mu_B/f.u.$ is obtained by the relation $C = N\mu_{eff}^2/3k_B$, where N is the number density of magnetic ions per unit gram, k_B is the Boltzmann's constant [13]. Because Li^+ and O^{2-} ions have no magnetic moment, the moment of $Li[Li_{0.2}Mn_{0.4}Ni_{0.4}]O_2$ originates from the magnetic transition metal ions. It has been reported that Ni and Mn ions in the sample will accept +3 and +4 [14], which will give spin only effective moment $1.73\mu_B$ and $3.87\mu_B$, respectively. So the theoretical effective moments of $Li[Li_{0.2}Mn_{0.4}Ni_{0.4}]O_2$ can be calculated to be $2.68(2)\mu_B$ by the

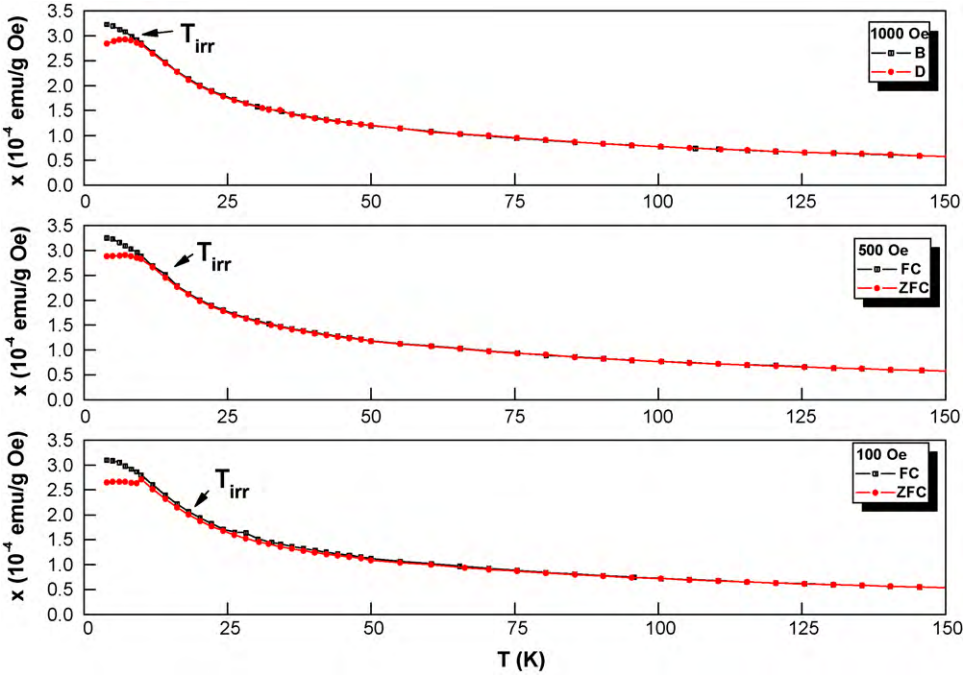

Fig. 3. ZFC and FC magnetization curves from 150 K to 4 K at a different magnetic field of 100 Oe, 500 Oe and 1000 Oe.

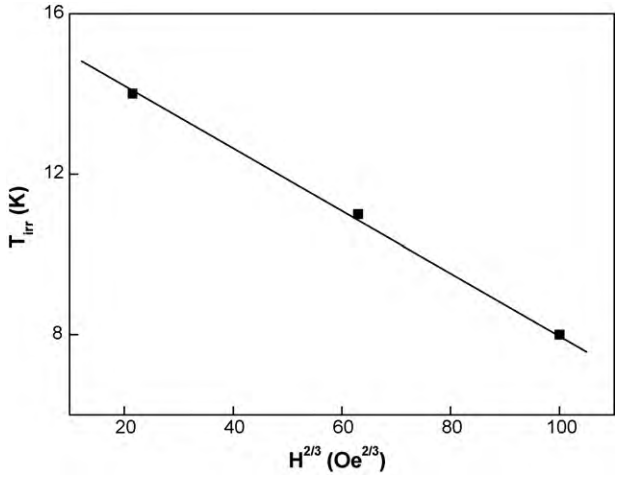

Fig. 4. Field dependence of the transition T_{irr}, as determined by the separation of ZFC and FC curves, showing the de Almeida–Thouless lines.

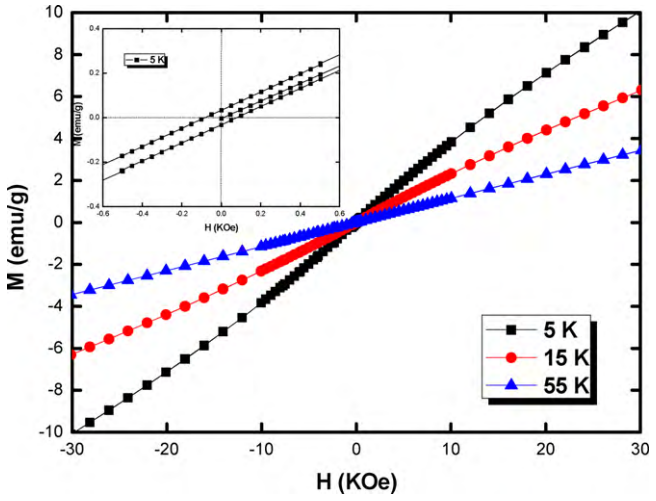

Fig. 5. The magnetic field variation of magnetization at different fixed temperature of 442 compound. The data have been taken with increasing and decreasing magnetic field. Maximum 5T magnetic field has been used.

equation $\mu_{eff} = \sqrt{0.4\mu^2_{Ni^{3+}} + 0.4\mu^2_{Mn^{4+}}}$. The coincidence between the experimental and theoretical moments not only confirm the valence state of Ni and Mn ions but also indicate the moments in this system are located on the magnetic ions.

Fig. 3 displays the *dc* magnetization from 150 K to 4 K in different applied magnetic field. The magnetization rises gradually with the decrease in temperature. At low temperature, the bifurcation between M_{ZFC} and M_{FC} indicates history dependence of the magnetization processes. The irreversibility magnetization, defined as $\Delta M = M_{FC} - M_{ZFC}$, can be used to identify the irreversibility temperature (T_{irr}) by $\Delta M \neq 0$. T_{irr} indicates the onset of the freezing process [15]. T_{irr} shifts to lower temperature with increase of applied field. Furthermore, the intensity of the broad peak in ZFC curve decreases with the applied field. These features suggest a spin-glass behavior of $Li[Li_{0.2}Mn_{0.4}Ni_{0.4}]O_2$ [16–18]. Furthermore, our *dc* magnetizations differ from that of the usual spin-glass behavior in that FC curve continues to rise for spin-glass-like (SGL) below T_{irr}, while the FC curve is almost flat for usual spin glass. The increase in the FC susceptibility below T_{irr} is due to the occurrence of the finite range of inhomogeneous state around a quasicritical temperature [16,19,20]. A similar magnetic behavior has been reported for SGL system [21,22,23].

The mean-field theory predicts one critical line in spin glass, which is called the de Almeida–Thouless (AT) line: [24]

$$H_{AT}(T_{irr})/_{\Delta}J_{\propto}(1 - T_{irr}/T_F)^{3/2}. \quad (1)$$

where T_F is the zero-field spin-glass freezing temperature and ΔJ is the width of the distribution of exchange interaction. As shown in Fig. 4, T_{irr} varies linearly with $H^{2/3}$, which indicates that our data satisfies the AT line. This finding confirms that $Li[Li_{0.2}Mn_{0.4}Ni_{0.4}]O_2$ exhibits the SGL behavior [24].

Fig. 5 shows the field dependence of magnetization at different temperatures. It is found that the lower the temperature, the more the $M(H)$ curve bends. However, the magnetic saturation is not observed with the applied magnetic field up to the 3 T. The magnetization becomes a nonlinear function of field and displays ferromagnetic behavior with a tiny hysteresis at low-field region, whose coercive field and remanence are 77.88 Oe and 0.032 emu/g at 5 K, respectively, as shown in the inset of Fig. 5. Both the absence of magnetization saturation at high-field region and the existence of hysteresis loop at low-field region are characteristics of SGL phase [25,26]. The Arrott plots are obtained from magnetization isotherms and shown in Fig. 6. No sign of the spontaneous magnetization can be seen, because there is a strong curvature toward the H/M axis and there is no intercept on the M^2 axis. The absence of the spontaneous magnetization indicates a short-range magnetic ordering [27], which is in consistence with the suggested SGL state.

In addition, it is interesting to discuss the magnetic behavior of $Li[Li_{(1/3-x/3)}Mn_{(2/3-2x/3)}Ni_x]O_2$ in comparison with that of rhombohedral $Li(Mn_xNi_{1-x})O_2$.

As reported in Ref. [28], the susceptibility of $Li(Mn_xNi_{1-x})O_2$ display a cusp in ZFC branch and a strong irreversibility behavior. SGL state has also been suggested for $Li(Mn_xNi_{1-x})O_2$ due to the random distribution between Ni and Mn ions at 3b sites. The system of $Li[Li_{(1/3-x/3)}Mn_{(2/3-2x/3)}Ni_x]O_2$ shows similar magnetic behavior in the line shape of ZFC/FC curve and irreversibility behavior, which can also be attributed to the SGL state at low temperature although there are some differences in the structure properties. The SGL ground state observed in $Li[Li_{(1/3-x/3)}Mn_{(2/3-2x/3)}Ni_x]O_2$ ($x = 0.4$) can be resulted from two reasons [10]: geometrical frustration and short-range structural disorder. Due to the triangular lattice in the TM layers, geometrical frustration usually induces interesting low-temperature magnetic behaviors such as isostructural compound $LiNiO_2$ [29,30]. A simple method to estimate the effect of geometrical frustration is to calculate frustration parameter $|\theta|/T_f$, where θ is Weiss constant and T_f is the peak temperature in the ZFC curve [30]. It is has been proposed that the condition, $|\theta|/T_f > 10$, is

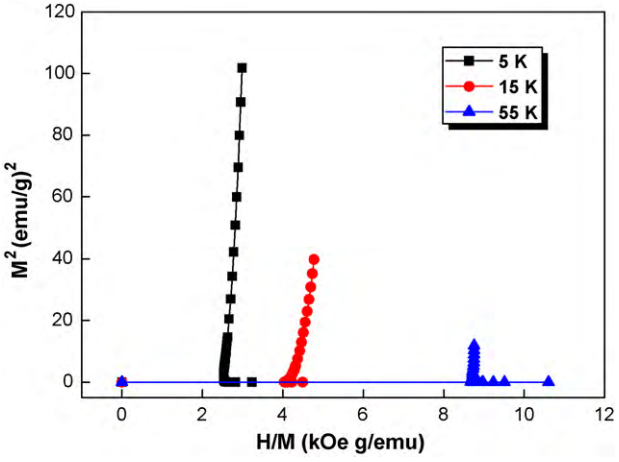

Fig. 6. Arrott plots (H/M vs M^2) using *dc* magnetization vs applied field taken at different fixed temperature for $Li[Li_{0.2}Mn_{0.4}Ni_{0.4}]O_2$.

taken as a criterion for the presence of frustration [31]. However, in $Li[Li_{0.2}Mn_{0.4}Ni_{0.4}]O_2$, the $|\theta|/T_f$ is calculated to be about 7.8, which is lower than the value that frustration is strong enough to give rise to the spin-glass in the system. We can conclude that geometrical frustration may not be the driving force for the formation of SGL. So the existence of SGL state may be mainly ascribed to the short-range structural disorder, especially the disorder arrangement of $Ni^{3+}/Li^{+}/Mn^{4+}$ ions in the TM layers and of Li^{+}/Ni^{3+} in 3a and 3b sites. Such kind of scenario of random distribution of ions in the lattice associated with the formation of spin-glass-like behavior has been found in the Cr-doped rhombohedral $LiMnO_2$ [23].

Acknowledgements

This work was sponsored by the Special Funds for Major State Basic Research Project of China under Grant No. 2009CB220104 and Program for Changjiang Scholar and Innovative Research Team in Jilin University and Grant No. IRT0625; supported by Supported by Research Fund for the Doctoral Program of Higher Education of China (new teacher) 20090061120020; supported by Jilin Project of Research and development No. 20075007.

References

[1] Z. Lu, J.R. Dahn, J. Electrochem. Soc. 149 (2002) A815–A822.
[2] J.-M. Kim, S. Tsuruta, N. Kumagai, Electrochem. Commun. 9 (2007) 103.
[3] A.D. Robertson, P.G. Bruce, Electrochem. Solid-State Lett. 7 (9) (2004) A294–A298.
[4] M.M. Thackeray, S.-H. Kang, C.S. Johnson, J.T. Vaughey, R. Benedek, S.A. Hackney, J. Mater. Chem. 17 (2007) 3112–3125.
[5] Y.J. Park, Y.-S. Hong, X. Wu, M.G. Kim, K.S. Ryu, S.H. Chang, J. Electrochem. Soc. 151 (2004) A720–A727.
[6] S.-H. Kang, K. Amine, J. Power Sources 124 (2003) 533–537.
[7] N.A. Chernova, M. Ma, J. Xiao, M.S. Whittinghan, J. Breger, C.P. Grey, Chem. Mater. 19 (2007) 4682–4693.
[8] J. Xiao, N.A. Cherrnova, M. Stanley, Wittingham, Chem. Mater. 20 (2008) 7454–7464.
[9] J.K. Ngala, N.A. Chernova, M. Ma, M. Mamak, Y. Peter, M. Zavalij, S. Whittingham, J. Mater. Chem. 14 (2004) 214–220.
[10] F. Du, X. Bie, Y. Chen, Y. Wei, L. Liu, C. Wang, G. Zou, G. Chen, J. Appl. Phys. 106 (2009) 053904.
[11] A. Andreanov, J.T. Chalker, T.E. Saunders, D. Sherrington, Phys. Rev. B 81 (2010) 014406.
[12] Z.-F. Huang, F. Du, C.-Z. Wang, D.-P. Wang, C. Chen, Phys. Rev. B 75 (2007) 054411.
[13] J. Sugiyama, H. Nozaki, J.H. Brewer, E.J. Ansaldo, G.D. Morris, C. Delmas, Phys. Rev. B 72 (2005) 144424.
[14] Y.-S. Hong, Y.J. Park, K.S. Ryu, S.H. Chang, M.G. Kim, J. Mater. Chem. 14 (2004) 1424–1429.
[15] B. Martinez, X. Obradors, L. Balcells, A. Rouanet, C. Monty, Phys. Rev. Lett. 80 (1998) 181.
[16] N. Marcano, J.C. Gomez Sal, J.I. Espeso, L. Fernadez Barquin, C. Paulsen, Phys. Rev. B 76 (2007) 224419.
[17] I.G. Deac, J.F. Mitchell, P. Schiffer, Phys. Rev. B 63 (2001) 172408.
[18] Takao Mori, Hiroaki Mamiya, Phys. Rev. B 68 (2003) 214422.
[19] Sunil Nair, A. Banerjee, Phys. Rev. Lett. 93 (2004) 117204.
[20] J.A. Mydosh, Spin Glasses: An Experimental Introduction, Taylor & Francis, London, 1993.
[21] A. Falqui, N. Lampis, A. G.-Lehmann, G. Pinna, J. Phys. Chem. B 109 (2005) 22967.
[22] S. Chatterjee, A.K. Nigam, Phys. Rev. B 66 (2002) 104403.
[23] F. Du, Z. Huang, C. Wang, X. Meng, G. Chen, Y. Chen, S. Feng, J. Appl. Phys. 102 (2007) 113906.
[24] M. Gruyters, Phys. Rev. Lett. 95 (2005) 077204.
[25] F. Wang, J. Zhang, Y.-F. Chen, G.-J. Wang, J.-R. Sun, S.-Y. Zhang, B.-G. Shen, Phys. Rev. B 69 (2004) 094424.
[26] Ya-Qiong Liang, Nai-Li Di, Zhao-Hua Cheng, Phys. Rev. B 72 (2005) 134416.
[27] R. Mathieu, P. Nordblad, D.N.H. Nam, N.X. Phuc, N.C. Khiem, Phys. Rev. B 63 (2001) 174405.
[28] Hironori Kobayashi, Hikari Sakaebe, Hiroyuki Kageyama, Kuniaki Tatsumi, Yoshinori Arachi, Takashi Kamiyama, J. Mater. Chem. 13 (2003) 590–595.
[29] E. Chappel, M.D. Nunez-Regueiro, S. de Brion, G. Chouteau, Phys. Rev. B 66 (2002) 132412.
[30] J.N. Reimers, J.R. Dahn, J.E. Greendan, C.V. Stager, G. Liu, I. Davidon, U. von Sacken, J. Solid State Chem. 102 (1993) 542.
[31] John E. Greedan, J. Mater. Chem. 11 (2001) 37–53.